International Journal of Mass Spectrometry 298 (2010) 17–23

Contents lists available at ScienceDirect

International Journal of Mass Spectrometry

journal homepage: www.elsevier.com/locate/ijms

Considerations in experimental and theoretical collision cross-section measurements of small molecules using travelling wave ion mobility spectrometry-mass spectrometry☆

Tom W. Knapman[a,b,c], Joshua T. Berryman[a,c], Iain Campuzano[d], Sarah A. Harris[a,c], Alison E. Ashcroft[a,b,*]

[a] Astbury Centre for Structural Molecular Biology, University of Leeds, Leeds LS2 9JT, UK
[b] Faculty of Biological Sciences, University of Leeds, Leeds LS2 9JT, UK
[c] School of Physics and Astronomy, University of Leeds, Leeds LS2 9JT, UK
[d] Waters MS Technologies Centre, Floats Road, Wythenshaw, Manchester M23 9LZ, UK

ARTICLE INFO

Article history:
Received 15 January 2009
Received in revised form
24 September 2009
Accepted 28 September 2009
Available online 4 October 2009

Keywords:
Ion mobility spectrometry
Cross-sectional area
Travelling wave ion guide
Mass spectrometry
Structural isomer

ABSTRACT

Travelling wave ion mobility spectrometry-mass spectrometry (TWIMS-MS) has the capability to separate ions based on their mobility through a gas-filled travelling wave (T-wave) device in the presence of a train of transient voltage pulses. By calibration of this device using analytes of previously determined cross-sectional area (from conventional IMS experiments), collision cross-sections of ions can be determined based on their drift time through the T-wave device. Comparison of experimentally determined cross-sections with theoretical calculations from structural models has the potential to provide methodology which can be applied to analytes of previously uncharacterised structure; however, this comparison relies on a high degree of confidence in both experimental and theoretical methods.

Focussing on small (≤200 Da) molecules, collision cross-sections have been measured by TWIMS-MS employing a calibration procedure that uses both oligo-glycine peptides and human haemoglobin-derived tryptic peptides in order to extend the calibration range for the measurement of high mobility ions. The effect of TWIMS wave height parameters on the calibration is addressed.

Theoretical TWIMS cross-section calculations have been performed using a rapid, Windows-based, in-house developed projection approximation algorithm. These estimates were optimised by comparison with experimental values for a series of small molecules with rigid core structures by systematic variation of the interaction radii of the atoms comprising these species until theoretical measurements were in agreement with experimentally derived TWIMS cross-sections. The effect of varying the interaction radius for the buffer gas was subsequently studied by comparison of theoretical collision cross-sections calculated using helium and nitrogen radii with TWIMS-MS cross-section measurements determined in either helium or nitrogen buffer gases. It was found that the buffer gas used in theoretical calculations should ideally match the buffer gas in which the cross-sections of the calibrants were originally determined by conventional IMS.

The resolving potential of the experimental methodology was demonstrated by separation of two isomeric amino acids, leucine and isoleucine, which showed <3% difference in cross-sectional areas. Furthermore, the application of both experimental and theoretical methods to compare the gas phase and solution conformations of seven amino acids was demonstrated. This study describes important considerations for the comparison of TWIMS-MS collision cross-sections with those obtained by theoretical methods, and also demonstrates that TWIMS-MS could be applied specifically to study a range of small molecules including those of pharmaceutical interest, in particular structural isomers and diastereoisomers that may not be distinguishable by mass spectrometry alone.

1. Introduction

The motion of a gas phase ion through a buffer gas in the presence of an electric field depends on both the charge of the ion and on its rotationally averaged cross-sectional area (Ω). Conventional ion mobility spectrometry (IMS) exploits this behaviour to facili-

☆ This article is part of a special issue on ion mobility.

* Corresponding author at: Astbury Building, Faculty of Biological Sciences, University of Leeds, Leeds LS2 9JT, UK. Tel.: +44 113 343 7273; fax: +44 113 343 7273.
E-mail address: a.e.ashcroft@leeds.ac.uk (A.E. Ashcroft).

1387-3806/$ – see front matter © 2009 Elsevier B.V. All rights reserved.
doi:10.1016/j.ijms.2009.09.011

tate the separation of ions by measurement of their drift time (t_D) through a gas-filled tube of defined length, and the technique can be interfaced to mass spectrometry (MS) to enable two-dimensional separations on the basis of mobility and mass-to-charge ratio [1]. IMS-MS may therefore be used to separate isomeric species of the same m/z ratio that are otherwise indistinguishable by MS alone [2], or provide an additional dimension of separation to complex samples, such as peptide mixtures generated by proteolytic digestion of proteins [3]. Additionally, IMS-MS can be used to measure the collision cross-section (Ω) of a given ion based on its mobility through the drift tube, using the fundamental relationship between cross-section and ion mobility at the low electric fields employed by the experiment [1]. By means of IMS cross-section measurements, there is the potential to gain information about the structure of ions: for example, the tertiary structures of co-populated protein conformers [4,5].

A recent development in the field of IMS has been travelling wave ion mobility spectrometry (TWIMS), where ions are accumulated and periodically released into a mobility 'T-Wave' cell, in which they separate according to their mobility through a continuous train of transient voltage pulses (travelling waves) after which they are analysed by time-of-flight MS [6]. Depending on the frequency of collisions with the buffer gas, ions are either carried along the drift cell and emerge with a short t_D, or fall back over the voltage potential and hence spend longer in the drift cell. Like conventional IMS, the mobility of an ion through the T-Wave cell depends on a number of factors, including the charge on the ion, the reduced mass between the ion and the buffer gas, the identity, pressure and temperature of the buffer gas and the collision cross-section of the ion [7,8].

Determination of collision cross-sections by TWIMS is a more complex process than for conventional IMS, given that the electric field experienced by the ions changes both temporally and spatially along the length of the drift cell, the result being that fundamental derivation of the relationship between mobility and drift time is highly complex [9]. In practice it is far easier to calibrate the T-Wave device using ions whose collision cross-sections have been previously determined by conventional IMS. Calibration is achieved generally by plotting a reduced cross-section (Ω'), which is directly proportional to mobility and is obtained by division of the literature cross-section by the absolute charge on the ion and its reduced mass with respect to the buffer gas, against the measured t_D [7,8,10,11]. The data are subsequently fitted to a linear or allometric function to obtain calibration coefficients from which a TWIMS cross-section of 'unknown' analytes can be derived after measurement of their t_D, which should be in good agreement with absolute cross-sections determined by conventional IMS-MS. Cross-section measurements of proteins [8,10], peptides [11], virus capsids [12] and commercial polymers [13] by this calibration method have been widely reported using tryptic peptides and/or both folded and unfolded proteins as calibrants [7,8], the cross-sections of which have been collated by Prof. David Clemmer (www.indiana.edu/~clemmer), based on several IMS cross-section measurements [14–16].

In order to gain useful information from measured cross-sections, the resemblance of gas phase ion structure to that in solution structure needs to be considered. This has been studied by comparison of experimentally derived cross-sections with those calculated from known structures obtained by NMR spectroscopy or X-ray diffraction [8,17]. The freely available MOBCAL software (www.indiana.edu/~nano) can be used to calculate cross-sections from a set of atomic coordinates and employs three different approaches to achieve this. The simplest calculation, the projection approximation (PA), calculates cross-section based on a hit/miss strategy between atoms in both the analyte and the buffer gas, each with a fixed interaction radii; the cross-sections of many two-dimensional snapshots covering the entire three-dimensional structure are calculated and the overall cross-section is taken as an average of these measurements [18]. The exact hard sphere scattering (EHSS) model computes a cross-section by modelling the analyte as an array of overlapping hard spheres with radii equal to hard sphere collision distances and calculating scattering angles of the buffer gas upon collision [19], while the more sophisticated trajectory method (TM) uses a similar approach to the EHSS algorithm, but models the interaction between the ion and the buffer gas as a Lennard-Jones potential [20,21].

The TM is generally considered to be the best representation of cross-section, since it models buffer gas–analyte interactions using a correct electrostatic potential, however the nature of these calculations means that the method is highly computationally expensive and hence is not applicable to large atom sets [14]. In the recent literature, it has been frequently demonstrated that the PA method generates cross-sections in good agreement with those experimentally derived for a wide range of analytes, however, it is suggested that buffer gas effects such as scattering angles need to be taken into account for larger ions with more complex concave shapes, as is achieved by the EHSS [14]. Despite this, there is still much variation throughout the literature in which method is applied to any particular analytes. Williams et al. report all three values for determining collision cross-sections of isomeric ruthenium complexes, although it is clear from the data that the PA and TM methods are in good agreement with each other, while the EHSS is significantly larger [22]. In contrast to this, Scarff et al. suggest that EHSS and TM produce similar results for the haemoglobin complex and that the PA gives an underestimate [17], while Faull et al. quote EHSS cross-sections alone in their study of cytochrome c [23]. Calculation of peptide cross-sections has been reported using the TM [3], and also an average of PA and EHSS values [14]. Thus, when considering a comparison between theoretical collision cross-section calculations with experimental values for previously uncharacterised analytes, it is sometimes unclear which MOBCAL program is the most appropriate to use.

In this study we demonstrate an approach that has enabled us to make ESI-TWIMS-MS collision cross-section measurements of high mobility, singly charged, small molecules and, in turn, to model TWIMS-derived cross-sections with empirically optimised theoretical cross-section calculations. These methods are of significance for all small molecule analyses, including those of pharmaceutical interest, and particularly the characterisation of structural isomers and diastereoisomers which have very little difference in collision cross-section and may not be resolvable using MS techniques alone. The methodology described involves a TWIMS cross-section calibration based on a series of oligo-glycine ions, whose cross-sections have been measured previously by conventional IMS-MS ([21] (www.indiana.edu/~clemmer)), which has been achieved with careful consideration of TWIMS parameters to optimise the separative power of the technique. The experimental method is supported by the empirical determination of gas phase interaction radii of carbon, hydrogen, oxygen and nitrogen atoms contained within small molecule structures with limited degrees of freedom by means of collision cross-section calculation using an improved version of an in-house adapted projection approximation algorithm [8]. The capability of this approach is illustrated by the separation of two isomeric amino acids. We subsequently show that our optimised theoretical methodology for predicting TWIMS cross-sections can be used to study the relationship between solution and gas phase structures of a range of amino acids by comparison of experimental values with those calculated from rotameric models of solution conformers.

2. Experimental

C_{60}, C_{70}, naphthalene, phenanthrene, pyrene, adamantane, amantadine, adamantane-1-carboxylic acid, leucine, isoleucine, proline, valine, glutamine, glutamic acid, aspartic acid, diglycine, triglycine, tetraglycine, pentaglycine, hexaglycine, human haemoglobin, bovine trypsin, ammonium acetate and caesium iodide were all obtained from Sigma Aldrich (Dorset, UK). Tryptic peptides were prepared as previously described [8,24]. The mobility calibrants and amino acids were prepared at 20 μM concentration in 10 mM ammonium acetate at pH 7, while all other analytes were analysed from toluene. Solvents were purchased from Fisher Scientific (Loughborough, UK).

Experiments were performed using a Synapt HDMS mass spectrometer (Waters UK Ltd., Manchester, UK), which has been described in detail elsewhere [6,24]. Mass spectra were acquired by positive nano-electrospray ionisation (ESI) using either thin-wall, gold-plated borosilicate vials (Waters UK Ltd., Manchester, UK) or a Nanospray Triversa (Advion Biosciences Corpn., Ithaca, NY, USA) interface. Mass calibration was achieved by separate infusion of caesium iodide (2 mg/mL, 1:1, v/v, H_2O:MeOH). The instrument was operated with a capillary voltage of 1.0 kV and a cone voltage of 30 V. The ion source block temperature was set to 70 °C. The Trap and Transfer T-Wave sections were operated at approximately 10^{-2} mbar of SF_6 and the ion mobility T-Wave at 3.00 mbar of helium, unless otherwise stated. The high pressure of helium in the central IMS T-Wave ion guide was achieved by replacing the standard 2 mm diameter apertures with 1 mm diameter apertures. The ion mobility T-Wave was operated with a wave velocity of 250 m/s with either a static pulse height of 4 V or a linear T-Wave ramp of 4–10 V. Data acquisition and processing were carried out using MassLynx (v4.1) software supplied with the instrument.

Drift time calibration of the T-Wave cell was achieved by separate infusion of a tryptic peptide mixture arising from human haemoglobin, and a test mix containing the five oligo-glycines. Drift times were used as recorded with corrections for mass dependent [7] and mass independent (0.9 ms; Dr. Kevin Giles, Waters UK Ltd., personal communication) flight times. Reduced cross-sections (Ω') were calculated from published cross-sections [14–16,21] and subsequently plotted against measured drift times (t_D). An allometric $y = Ax^B$ fit was applied to the data to yield calibration coefficients. Experimental cross-sections were determined by separate infusion of each analyte and measurement of the drift time centroid for the molecular-related ions by means of Gaussian fitting to the drift time distribution.

Computational cross-sections were calculated from Protein Data Bank (PDB) format structures using a rapid windows-based algorithm scripted in C (Leeds Method) translated from the MATLAB code as previously reported [8]. This algorithm is capable of yielding cross-sections within a few seconds from unprocessed PDB files. Structures of small molecules were modelled using PyMol (DeLano Scientific, San Carlos, CA, USA). Interaction radii of the buffer gas and the atoms within the PDB file were collated in a reference file for easy access to edit and so different radii could be used in the calculations to obtain the best fit with the TWIMS measured cross-sections. Cross-sections were averaged over 20×20 snapshots in the θ and φ axes. Calculations were made using 1.40 Å for the interaction radius of the helium buffer gas, obtained from the reported van der Waals radius of monoatomic helium [25]. The radius of N_2 buffer gas, 1.80 Å, was obtained from calculation of the cross-section of an ellipse based on the van der Waals radius of monoatomic nitrogen (1.55 Å) [25] and the bond length of a N—N triple bond of 1.1 Å [26]. Empirical atomic interaction radii were determined by systematic variation of the atom of interest for each small molecule until agreement between the experimental and calculated cross-sections was observed.

Amino acid cross-sections were calculated using PDB structures generated from the penultimate rotamer library derived by the Richardson laboratory (http://kinemage.biochem.duke.edu/databases/rotamer.php) using a database of high-resolution X-ray structures [27]. Cross-sections reported for each amino acid were calculated as a weighted average over all rotameric conformers.

3. Results and discussion

3.1. ESI-TWIMS-MS collision cross-section calibration for ions of high mobility

The general guidelines for ESI-TWIMS-MS operation [7,8,24], and for calibrating collision cross-sections from the recorded TWIMS drift-times by comparison with collision cross-sections measured elsewhere for the same analytes (www.indiana.edu/~clemmer) using conventional IMS-MS instrumentation [7,8] have been detailed previously.

A comparison of the calibration curves arising from setting different T-Wave conditions using di-, tri-, tetra-, penta- and hexaglycine (reported (www.indiana.edu/~clemmer) Ωs 62, 76, 86, 97, and 107 Å^2, respectively) and haemoglobin-derived tryptic peptides as calibrants is shown in Fig. 1. During each individual (18 ms) mobility experiment, the 300 ms^{-1} T-wave amplitude was either held at a static 4 V wave or ramped from 4–10 V. From Fig. 1 it can be seen that the Ω', and hence the mobility range, covered by the calibration is significantly extended at the higher mobility end by the inclusion of the oligo-glycine calibration points, and is thus highly suitable for the collision cross-section calculations of singly charged, small molecules as it avoids the need for calibration extrapolation that would be necessary with a calibration based merely on tryptic peptides or unfolded proteins alone [7,8,10]. Indeed, the inclusion of the high-mobility oligo-glycine calibrants extends the TWIMS calibration from a lower calibration limit of $\Omega' \sim 1.3 \times 10^{21}$ Å^2 Da^{-1} C^{-1} using the smallest singly charged tryptic peptide of haemoglobin reported [14], to $\sim 7.5 \times 10^{20}$ Å^2 Da^{-1} C^{-1}. As the small molecule analytes studied in this project fall into this high mobility calibration range, an extended calibration range is essential. It is also interesting to note that the two T-wave conditions employed produce significantly different calibration characteristics: the 4–10 V wave ramp conditions yield a calibration that covers a wide range of Ω' values, corresponding to a cross-section range for singly charged ions

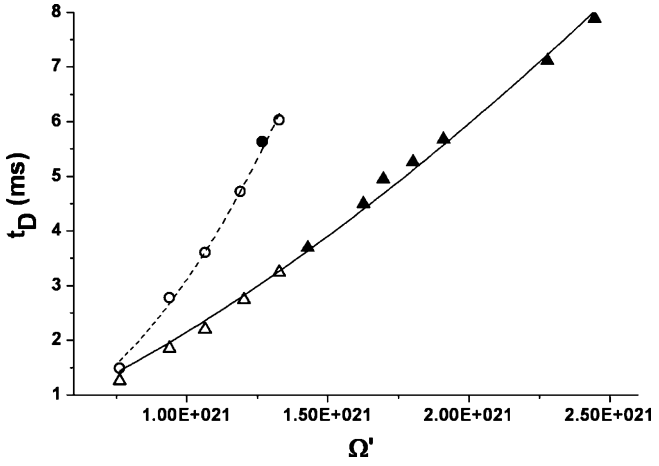

Fig. 1. ESI-TWIMS-MS calibration curves for oligo-glycine (open) and tryptic haemoglobin peptides (filled) at two different T-wave settings: a 4–10 V ramp (triangles) and a static 4 V wave (circles). The solid and dotted lines represent an allometric fit to each dataset.

of approximately 60–200 Å^2, thus providing a generic calibration for small molecule collision cross-section measurements with a range of Ω' values. Conversely, the static 4 V wave resolves a relatively limited Ω' range over the drift time scale making this calibration more specific to analytes within this range, offering potentially better resolving power. Under the static 4 V wave conditions, haemoglobin-derived tryptic peptides with Ω' values larger than that of hexaglycine (1.33×10^{21} Å^2 Da^{-1} C^{-1}) are observed to have drift time distributions that "roll-over" the T-wave into the subsequent IMS scan and therefore cannot be used for calibration.

3.2. Calculating collision cross-sections for comparison with ESI-TWIMS-MS data

In order to compare TWIMS-measured, gas phase collision cross-sections with solution cross-sections, and thus gain confidence in this approach when applying it to previously uncharacterised molecules, we have developed [8] and subsequently refined an algorithm (Leeds Method) based on the simplest MOBCAL projection approximation (PA) calculation. This algorithm now shows significant improvement over the original MOBCAL code in terms of computational speed, ease of use, flexibility of input file format and compatibility with Windows operating systems. In order to optimise the performance of our PA calculation with respect to the more sophisticated trajectory method, we have included variable atomic interaction radii in the user interface. This permits empirical optimisation of the calculated cross-sections of analytes of known structures, with the overall aim of enabling meaningful predictions of TWIMS-derived cross-sections, and hence structural insights, for previously uncharacterised species.

In order to study atomic radii, the 4–10 V voltage ramp was employed in the analysis of an array of small, compact molecules depicted in Fig. 2, chosen on the basis of their atomic composition so as to enable sequential determination of empirical gas phase interaction radii for these atoms. It was also important to select analytes without freely roatable bonds in their core structure, i.e., with limited degrees of freedom, to limit the variability in structure upon transference into the gas phase.

The series of small molecules began with fullerenes C_{60} and C_{70} for the determination of the carbon interaction radius (r_C), since they are well-defined, discrete structures containing only carbon atoms [28]. Following this, the hydrogen interaction radius (r_H) was studied using a series of polycyclic, fused arenes, in addition to the diamondoid compound, adamantane. Further studies involving the oxygen and nitrogen radii (r_O and r_N respectively), were undertaken using substituted adamantane derivatives. Table 1 shows the sequential process by which the interaction radii were determined, along with the measured and calculated cross-sections for each molecule.

The agreement between the ESI-TWIMS-MS measured and Leeds Method calculated Ω values for both C_{60} and C_{70} is optimum (<1% difference) when calculated with $r_C = 1.38$ Å (Table 1). This value was determined as the average of the individual empirically derived values for C_{60} and C_{70}, and the C_{60} value was in good agreement with that previously published (120–130 Å^2) [29]. Atomic radii reported in literature vary widely depending on the methodology of determination [30]. Usually this involves quantum mechanical calculations [30] or empirical derivation [31]. The value of 1.38 Å obtained in this study is significantly smaller than typically calculated carbon radii of ~1.70 Å [25], which gave cross-sections for C_{60} and C_{70} of 132.60 and 144.56 Å^2, respectively, compared with the values of 119.34 and 131.83 Å^2 measured in this TWIMS experiment. This suggests that the interaction radii in the gas phase are somewhat smaller than the reported solution radii for these

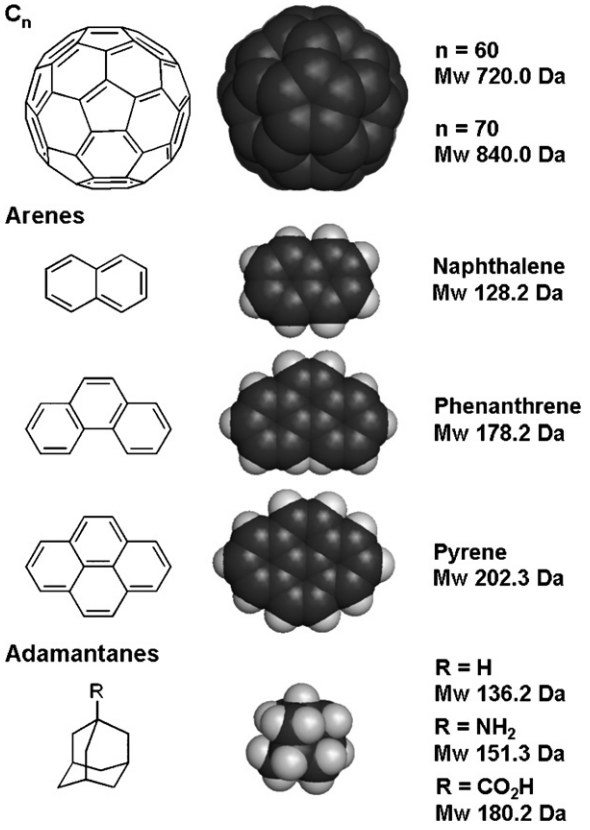

Fig. 2. Structures and "space filling" models of the small molecules used for ESI-TWIMS-MS optimisation of atomic interaction radii.

atoms. Using the r_C value derived from the fullerene data, the cross-sections of different rigid arene structures and the diamondoid, adamantane were calculated using the Leeds Method while systematically varying r_H until agreement with the experimentally derived cross-section was observed.

Determination of the r_H gave anomalous results with respect to the very different structures of the aromatic arene series and the aliphatic cage-like adamantine. Carrying through $r_C = 1.38$ Å from the fullerene data gave the best fit to within 1% for the three arenes using the average of their empirically derived values, $r_H = 0.93$ Å. However, using $r_C = 1.38$ Å and $r_H = 0.93$ Å gave a ~10% overestimate for the cross-section calculation of adamantane, which only reached agreement with the experimental, TWIMS cross-section of 62.62 Å^2 when a value of $r_H = 0.72$ Å was used. Interestingly, although using $r_H = 0.72$ Å gave excellent agreement, changing r_C between 1.20 and 1.60 Å while keeping $r_H = 0.72$ Å did not produce any significant variation in the agreement with the cross-sectional area. This suggests that within the conditions of this comparison, r_H varies depending on the bonded environment of the hydrogen atom, which is consistent with published parameterisation of atomic radii in solution, where smaller r_H radii are calculated in aliphatic systems in comparison with aromatic-bonded protons [32]. Therefore, an aromatic or aliphatic r_H of 0.93 and 0.73 Å, respectively were used in subsequent cross-section calculations. Interaction radii r_O and r_N were estimated from the analysis of substituted adamantane compounds, averaging for σ- and π-bonded oxygen over the resonance-stabilised carboxylic acid group. All determined cross-sections for these species were found to be in good agreement with the MOBCAL Trajectory Method, while the MOBCAL Projection Approximation gave more varied results, predicting cross-sections smaller than our measured and predicted

Table 1
Sequential determination of interaction radii r_x (x = carbon, hydrogen, nitrogen and oxygen), by comparison between experimental ESI-TWIMS-MS collision cross-sections (Ω_{Exp}) and cross-sections calculated by the Leeds Method with the specified radii (Ω_{Theory}). In each case, one atom type is studied (shaded grey), and the subsequent interaction radius carried through to the next molecule.

	r_H (Å)	r_C (Å)	r_H (Å)	r_N (Å)	r_O (Å)	Ω_{Theory} (Å^2)	Ω_{Exp} (Å^2)	$\Omega_{mobcal\ PA}$ (Å^2)	$\Omega_{mobcal\ TM}$ (Å^2)
C_{60}	1.40	1.38				119.97	119.34	116.79	123.09
C_{70}	1.40	1.38				131.51	131.83	127.03	132.42
Naphthalene $C_{10}H_8$	1.40	1.38	0.93			61.57	60.07	63.61	60.92
Phenanthrene $C_{14}H_{10}$	1.40	1.38	0.93			71.98	72.08	76.78	72.76
Pyrene $C_{16}H_{10}$	1.40	1.38	0.93			74.67	76.57	80.39	72.76
Adamantane $C_{10}H_{16}$	1.40	1.38	0.72[a]			62.62	62.62	64.34	63.37
Amantadine $C_{10}H_{17}N$	1.40	1.38	0.72[a]	1.43		66.40	66.40	66.94	66.28
Adamantane-1-carboxylic acid $C_{11}H_{16}O_2$	1.40	1.38	0.72[a]		1.61	70.97	70.97	70.95	70.25

[a] The r_H value determined for adamantane is carried through to its subsequent derivative. The collision cross-sections calculated using the MOBCAL projection approximation ($\Omega_{mobcalPA}$) and the MOBCAL trajectory method ($\Omega_{mobcalTM}$) are also included.

values for fullerene structures but larger cross-sections for the arene series (Table 1).

3.3. Buffer gas considerations

A fundamental property of collision cross-sections is their dependence on the IMS buffer gas in which they are measured: the larger the buffer gas molecules, the larger the collision cross-section. Theoretically, a given ESI-TWIMS-MS calibration should only yield cross-sections comparable to absolute values measured in conventional IMS if performed in the same buffer gas in which the pre-determined cross-sections were originally measured. Using the ramped 4–10 V calibration graph acquired in helium buffer gas (Fig. 1), the collision cross-sections of the three arene compounds (Fig. 2) in 0.5 mbar of nitrogen gas were determined under otherwise identical ESI-TWIMS-MS instrumental conditions. Fig. 3a shows ESI m/z spectra of the three species.

Fig. 3b shows the mobility (t_D) chromatograms acquired for naphthalene, phenanthrene and pyrene acquired in helium buffer gas, together with their TWIMS experimental collision cross-

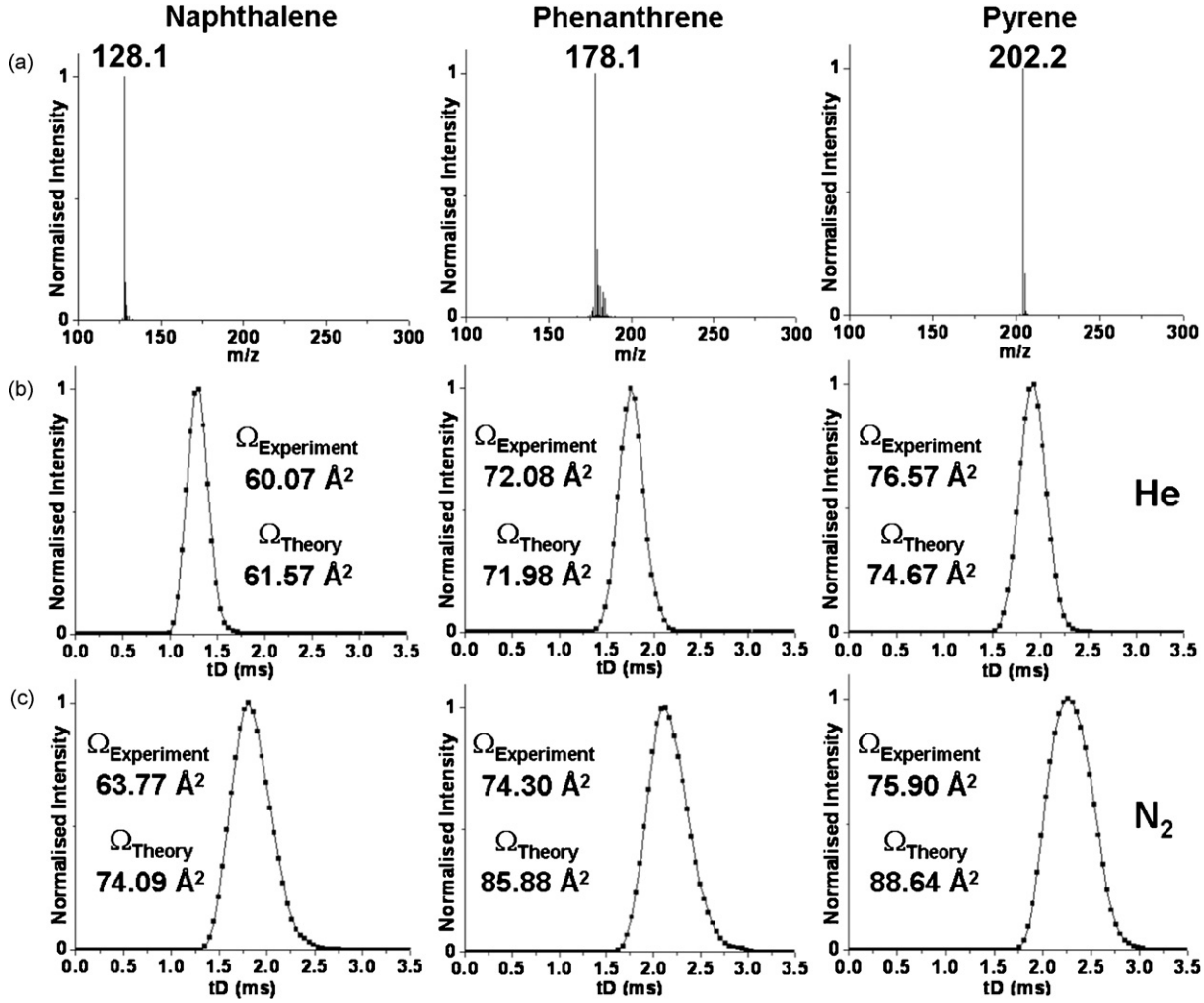

Fig. 3. ESI-TWIMS-MS data for naphthalene, phenanthrene and pyrene. (a) Nano-ESI m/z spectra showing molecular-related ions; (b) Mobility (t_D) chromatograms acquired in helium buffer gas; (c) Mobility (t_D) chromatograms acquired in nitrogen buffer gas. The ESI-TWIMS-MS measured and theoretically calculated collision cross-section areas for each species in each buffer gas are indicated.

sections based on the oligo-glycine and haemoglobin tryptic peptide calibrants (the cross-sections of which were derived by conventional IMS also using helium as a buffer gas) as described above. The Leeds Method-calculated cross-sections are also noted on the figure; these are the cross-sections for the three analytes using a helium gas radius of 1.40 Å [25] and the empirically derived interaction radii, r_C and aromatic r_H, of 1.38 and 0.93 Å, respectively.

Fig. 3c shows the mobility (t_D) chromatograms of the three arenes acquired using nitrogen buffer gas. The oligo-glycine and haemoglobin tryptic peptide calibrants were also analysed in nitrogen buffer gas by TWIMS-MS and a calibration curve constructed using the reported cross-sections derived in helium from conventional IMS experiments. The theoretical cross-sections shown were calculated again using r_C and r_H of 1.38 and 0.93 Å, but this time using a nitrogen buffer gas radius of 1.80 Å [25].

Agreement between experimental and calculated TWIMS collision cross-sections in Fig. 3b for the data acquired using helium as a buffer gas is absolute, since the experimental cross-section was used to optimise the radii used in the calculation. The calculated cross-sections in Fig. 3c, using the nitrogen gas radius of 1.80 Å, however, are consistently larger than the experimental values, which are in better agreement with the experimental and theoretical cross-sections in Fig. 3b derived using helium buffer gas. This important observation can be explained by the fact that the longer drift times observed using the larger nitrogen molecules as the buffer gas have been corrected to the helium cross-sections measured by conventional IMS in the calibration procedure and hence the cross-sections measured experimentally by ESI-TWIMS-MS are in agreement with those measured using helium buffer gas. This is an important consideration when comparing theoretically and experimentally derived TWIMS cross-sections in different buffer gases: the buffer gas radius used in the theoretical calculations must be indicative of the buffer gas used originally for conventional IMS derivation of the cross-sections employed in the calibration, even if the analysis of the calibrants and the analytes is carried out in a different buffer gas.

3.4. Using ESI-TWIMS-MS to separate small molecule structural isomers

As a validation of the improved, small molecule TWIMS methodology, the isomeric amino acids leucine and isoleucine (131 Da) were analysed by ESI-TWIMS-MS to determine whether both the experimental (TWIMS resolution and calibration procedure) and the theoretical (algorithm parameter sets) methods could distinguish between two isomeric compounds with an assumed minimal difference in cross-section. Fig. 4 shows the overlaid mobility (t_D) chromatograms for leucine and isoleucine measured using the higher resolution calibration with a static T-wave height of 4 V. Isoleucine was found to have a consistently higher mobility/shorter t_D and indicated a TWIMS-MS collision cross-section of 68.95 Å^2, compared with 70.51 Å^2 measured for leucine (Table 2). Thus, under these conditions, collision cross-section measurements with a difference in cross-section of <3% are feasible.

To demonstrate the capability of the theoretical approach for predicting TWIMS cross-sections with optimised radii, the relationship between solution and gas phase conformations for a series of amino acids with varying degrees of side-chain flexibilities and chemical properties was investigated. TWIMS collision cross-sections were determined using the calibration procedure with a static T-wave voltage, and theoretical cross-sections were calculated as a weighted average over multiple rotameric states from a database of 500 protein structures [27]. Table 2 shows TWIMS-MS experimental and Leeds Method theoretical TWIMS cross-sections for seven amino acids, together with the differences between the two values.

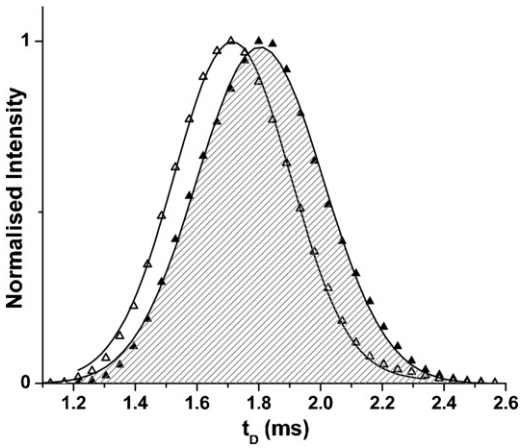

Fig. 4. Overlaid mobility chromatograms of isoleucine (open) and leucine (filled) acquired using a static 4 V wave height. The ESI-TWIMS-MS experimental collision cross-sections measured were 68.95 and 70.51 Å^2, and the calculated collision cross-sections were 70.81 and 72.03 Å^2, for isoleucine and leucine, respectively.

The first observation from these data is that close agreement (within 2–3%) between the TWIMS experimental and theoretical cross-sections is observed for amino acids with hydrophobic side-chains, while the experimental TWIMS cross-sections are significantly (~20%) smaller than the predicted theoretical cross-sections from the solution rotamers for amino acids with polar side-chains. Furthermore, it can be seen that the agreement between the solution conformers and the gas phase measured values varies as a function of side-chain length and chemical structure. The calculated cross-sections for proline and valine, both of which have limited degrees of side-chain freedom, give the best agreement with experimental TWIMS cross-sections, while the slightly larger leucine and isoleucine are smaller in the gas phase by 2–3%. The polar side-chains display a more significant trend, with aspartic acid showing less reduction in the gas phase than the longer side-chain analogues glutamic acid and glutamine. This study indicates that the conformations adopted by amino acids in the gas phase are highly dependent both on the chemical and structural properties of their side-chains: residues with polar side-chains are significantly smaller than expected, most likely due to interactions with the polar and charged termini, while hydrophobic residues bear greater resemblance to their solution counterparts, which is in agreement with published data on the intrinsic sizes of amino acids within peptide chains suggesting that non-polar residues adopt more extended conformations in the gas phase than polar ones [33]. This trend has also been seen in the conventional IMS cross-section measurements of the dipeptides LK and KK of 100.92 and 97.40 Å^2, respectively [34] (www.indiana.edu/~clemmer), The data also suggest that the degree of reduction in cross-section depends on the degrees of freedom in the side-chain.

Table 2
Experimental ESI-TWIMS-MS and theoretically derived collision cross-sections for seven naturally occurring amino acids, together with the difference between the two values. Theoretical collision cross-section determination was performed on a series of calculated rotamers [27]. The number of rotamers for each amino acid is shown. Residues with non-polar side-chains are shaded grey.

Amino acid	M_w (Da)	Rotamers	Ω_{Exp} (Å^2)	Ω_{Theory} (Å^2)	Difference
Leu	131.12	4	70.51	72.03	1.52
Ile	131.12	4	68.95	70.81	1.86
Pro	115.13	2	62.43	63.16	0.73
Val	117.15	3	64.81	64.82	0.01
Asp	133.11	5	62.93	69.81	6.88
Gln	146.15	5	62.85	75.08	12.23
Glu	147.13	7	63.35	76.69	13.34

4. Conclusion

This study demonstrates several important factors that need to be considered in any TWIMS-MS experiment with respect to cross-section calibration, instrumental parameters, buffer gas composition, and the calculation of theoretical cross-sections from known structures. First, the use of oligo-glycine calibrants shows how a rational choice of calibrants based on the high mobility range of the analytes can yield accurate experimental cross-sections, avoiding the need to extrapolate beyond the limits of the generally used calibration. Selection of suitable T-wave conditions can be employed to study a range of analytes with different cross-sections using ramped T-wave heights, or alternatively to study a single species, or species with very similar cross-sections such as structural isomers, to a higher resolution by using a static T-wave height.

It is possible to make good predictions of TWIMS-measured cross-sections of small molecules using the optimised Leeds Method algorithm incorporating empirical gas phase radii for different atoms. It should be taken into consideration, however, that if calibration and measurement of analyte drift times is performed – in any buffer gas – using calibrants whose cross-sections have previously been determined in helium using conventional IMS, any theoretical calculations undertaken for comparison with experimental cross-sections should be performed assuming a helium buffer gas interaction radius.

It has also been demonstrated that ESI-TWIMS-MS has the potential to measure the collision cross-sections of small molecules, and also that it has the capability to separate isomeric species based on a small difference in mobilities. This is likely to be significant for the analysis of pharmaceutically relevant species and small molecule forenscis, particularly if dealing with structural isomers or diastereoisomers. A study of amino acid conformations in the gas phase with respect to their structural and chemical properties has been made to illustrate how the comparison between experimentally measured and theoretically derived cross-sections can yield information on gas phase structure.

Acknowledgements

T.W.K. and J.T.B. are funded by post-graduate awards from the White Rose Doctoral Training Centre and the EPSRC. We thank James Muldoon from the School of Chemistry, University of Leeds for samples of adamantane and its derivatives. We also thank the BBSRC for financial support for instrumentation.

References

[1] A.B. Kanu, P. Dwivedi, M. Tam, L.M. Matz, H.H. Hill, Ion mobility-mass spectrometry, J. Mass Spectrom. 43 (2008) 1–22.
[2] P. Dwivedi, C. Wu, L.M. Matz, B.H. Clowers, W.F. Siems, H.H. Hill, Gas-phase chiral separations by ion mobility spectrometry, Anal. Chem. 78 (2006) 8200–8206.
[3] L. Tao, J.R. McLean, J.A. McLean, D.H. Russell, A collision cross-section database of singly-charged peptide ions, J. Am. Soc. Mass Spectrom. 18 (2007) 1232–1238.
[4] D.E. Clemmer, R.R. Hudgins, M.F. Jarrold, Naked protein conformation: cytochrome c in the gas phase, J. Am. Chem. Soc. 117 (1995) 10141–10142.
[5] D.E. Clemmer, M.F. Jarrold, Ion mobility measurements and their applications to clusters and biomolecules, J. Mass Spectrom. 32 (1997) 577–592.
[6] K. Giles, S.D. Pringle, K.R. Worthington, D.R. Little, J.L. Wildgoose, R.H. Bateman, Applications of a travelling wave-based radio-frequency-only stacked ring ion guide, Rapid Commun. Mass Spectrom. 18 (2004) 2401–2414.
[7] B. Ruotolo, J.L. Benesch, A.M. Sandercock, S.-J. Hyung, C.V. Robinson, Ion mobility-mass spectrometry analysis of large protein complexes, Nat. Protocols 3 (2008) 1139–1152.
[8] D.P. Smith, T.W. Knapman, I. Campuzano, R.W. Malham, J.T. Berryman, S.E. Radford, A.E. Ashcroft, Deciphering drift time measurements from travelling wave ion mobility spectrometry-mass spectrometry, Euro. J. Mass Spectrom. 15 (2009) 113–130.
[9] A.A. Shvartsburg, R.D. Smith, Fundamentals of traveling wave ion mobility spectrometry, Anal. Chem. 80 (2008) 9689–9699.
[10] C.A. Scarff, K. Thalassinos, G.R. Hilton, J.H. Scrivens, Travelling wave ion mobility mass spectrometry studies of protein structure: biological significance and comparison with X-ray crystallography and nuclear magnetic resonance spectroscopy measurements, Rapid Commun. Mass Spectrom. 22 (2008) 3297–3304.
[11] K. Thalassinos, M. Grabenauer, S.E. Slade, G.R. Hilton, M.T. Bowers, J.H. Scrivens, Characterisation of phosphorylated peptides using travelling wave-based and drift cell ion mobility mass spectrometry, Anal. Chem. 81 (2009) 248–254.
[12] C. Uetrecht, C. Versluis, N.R. Watts, P.T. Wingfield, A.C. Steven, A.J.R. Heck, Stability and shape of hepatitis B virus capsids in vacuo, Angew. Chemie I. E. 47 (2008) 6247–6251.
[13] J.P. Williams, J.H. Scrivens, Coupling desorption electrospray ionisation and neutral desorption/extractive electrospray ionisation with a travelling-wave based ion mobility mass spectrometer for the analysis of drugs, Rapid Commun. Mass Spectrom. 22 (2008) 187–196.
[14] S.C. Henderson, S.J. Valentine, A.E. Counterman, D.E. Clemmer, ESI/ion trap/ion mobility/time-of-flight mass spectrometry for rapid and sensitive analysis of biomolecular mixtures, Anal. Chem. 70 (1999) 291–301.
[15] C.S. Hoaglund-Hyzer, S.J. Valentine, C.R. Sporleder, J.P. Reilly, D.E. Clemmer, Three-dimensional ion mobility/TOFMS analysis of electrosprayed biomolecules, Anal. Chem. 70 (1998) 2236–2242.
[16] K.B. Shelimov, D.E. Clemmer, R.R. Hudgins, M.F. Jarrold, Protein structure in vacuo: gas-phase conformations of BPTI and cytochrome c, J. Am. Chem. Soc. 119 (1997) 2240–2248.
[17] C.A. Scarff, V.J. Patel, K. Thalassinos, J.H. Scrivens, Probing hemoglobin structure by means of traveling-wave ion mobility mass spectrometry, J. Am. Soc. Mass Spectrom. 20 (2009) 625–631.
[18] G. von Helden, M.-T. Hsu, N. Gotts, M.T. Bowers, Carbon cluster cations with up to 84 atoms: structures, formation mechanism and reactivity, J. Phys. Chem. 97 (1993) 8182–8192.
[19] A.A. Shvartsburg, M.F. Jarrold, An exact hard-spheres scattering model for the mobilities of polyatomic ions, Chem. Phys. Lett. 261 (1996) 86–91.
[20] M.F. Mesleh, J.M. Hunter, A.A. Shvartsburg, G.C. Schatz, M.F. Jarrold, Structural information from ion mobility measurements: effects of the long-range potential, J. Phys. Chem. 100 (1996) 16082–16086.
[21] T. Wyttenbach, J.E. Bushnell, M.T. Bowers, Salt bridge structures in the absence of solvent? The case for oligoglycines, J. Am. Chem. Soc. 120 (1998) 5098–5103.
[22] J.P. Williams, T. Bugarcic, A. Habtemariam, K. Giles, I. Campuzano, P.M. Rodger, P.J. Sadler, Isomer separation and gas-phase configurations of organoruthenium anticancer complexes: ion mobility mass spectrometry and modeling, J. Am. Soc. Mass Spectrom. 20 (2009) 1119–1122.
[23] P.A. Faull, K.E. Korkeila, J.M. Kalapothakis, A. Gray, B.J. McCullough, P.E. Barran, Gas-phase metalloprotein complexes interrogated by ion mobility-mass spectrometry, Int. J. Mass Spectrom. 283 (2009) 140–148.
[24] S.D. Pringle, K. Giles, J.L. Wildgoose, J.P. Williams, S.E. Slade, K. Thalassinos, R.H. Bateman, M.T. Bowers, J.H. Scrivens, An investigation of the mobility separation of some peptide and protein ions using a new hybrid quadrupole/travelling wave IMS/oa-ToF instrument, Int. J. Mass Spectrom. 261 (2007) 1–12.
[25] A. Bondi, Van der Waals volumes and radii, J. Phys. Chem. 68 (1964) 441–451.
[26] G. Menconi, D.J. Tozer, Diatomic bond lengths and vibrational frequencies: assessment of recently developed exchange-correlation functionals, Chem. Phys. Lett. 360 (2002) 38–46.
[27] S.C. Lovell, J.M. Word, J.S. Richardson, D.C. Richardson, The penultimate rotamer library, Proteins: Struct. Funct. Genet. 40 (2000) 389–408.
[28] H.W. Kroto, J.W. Heath, S.C. O'Brien, R.F. Curl, R.E. Smalley, C60: Buckminsterfullerene, Nature 318 (1985) 162–163.
[29] T. Wyttenbach, G. Von Helden, J.J. Batka, D. Carlat, M.T. Bowers, Effect of the long-range potential on ion mobility measurements, J. Am. Soc. Mass Spectrom. 8 (1997) 275–282.
[30] B. Zhou, M. Agarwal, C.F. Wong, Variable atomic radii for continuum-solvent electrostatics calculation, J. Chem. Phys. 129 (2008) 014509/1–014509/9.
[31] E.V. Stefanovich, T.N. Truong, Optimized atomic radii for quantum dielectric continuum solvation models, Chem. Phys. Lett. 244 (1995) 65–74.
[32] D. Tannor, B. Marten, R. Murphy, R.A. Friesner, D. Sitkoff, A. Nicholls, B. Honig, M. Ringnalda, W.A. Goddard, Accurate first principles calculation of molecular charge distributions and solvation energies from Ab Initio quantum mechanics and continuum dielectric theory, J. Am. Chem. Soc. 116 (2002) 11875–11882.
[33] S.C. Henderson, J. Li, A.E. Counterman, D.E. Clemmer, Intrinsic size parameters for Val, Ile, Leu, Gln, Thr, Phe, and Trp residues from ion mobility measurements of polyamino acid ions, J. Phys. Chem. B 103 (1999) 8780–8785.
[34] S.J. Valentine, A.E. Counterman, C.S. Hoaglund-Hyzer, D.E. Clemmer, Intrinsic amino acid size parameters from a series of 113 lysine-terminated tryptic digest peptide ions, J. Phys. Chem. B 103 (1999).